INTERNATIONAL ATOMIC ENERGY AGENCY
UNITED NATIONS EDUCATIONAL, SCIENTIFIC AND CULTURAL ORGANIZATION
INTERNATIONAL CENTRE FOR THEORETICAL PHYSICS
I.C.T.P., P.O. BOX 586, 34100 TRIESTE, ITALY, CABLE: CENTRATOM TRIESTE

SMR.550 - 22

SPRING COLLEGE IN MATERIALS SCIENCE ON
"NUCLEATION, GROWTH AND SEGREGATION IN MATERIALS
SCIENCE AND ENGINEERING"
(6 May - 7 June 1991)

STABILITY OF MICROSCOPIC CLUSTERS

(PART V)

J.A. ALONSO
Departamento de Fisica Teorica y Fisica Atomica
Molecular y Nuclear
Facultad de Ciencias
Universidad de Valladolid
47011 Valladolid
Spain

STABILITY OF MICROSCOPIC CLUSTERS

5th Lecture: Non-metallic clusters

J. A. ALONSO

Lectures to be delivered at:
Spring College in Materials Science on
"Nucleation, growth and segregation in Materials Science and Engineering"
(International Centre for Theoretical Physics, Triestre, May-June 1991)

1. INTRODUCTION

In the last Lecture of this Series I will briefly review some miscellaneous topics of interest concerning non metallic clusters.

2. CLUSTERS OF IONIC MATERIALS: ALKALI HALIDES[1-3]

In the mixture of positive ions and conduction electrons it is the wave-like electrons that dominate the properties of metal clusters as a whole.

A salt like NaCl is also a very simple mixture. It is composed of spherical closed-shell ions, Na^+ and Cl^-, both heavy, particle-like building blocks. It may therefore be expected to grow in analogy to Xenon clusters. The cohesion is due to monopole Coulomb forces, so it is more strongly bound than Xenon, where the binding is due to van der Waals forces. In addition there are two components, not one, and this actually prevents a close analogy to Xenon with its icosahedral shell structure.

The growth spiral in figure 1 of Lecture 1 shows in detail the picture one has of the first thirteen steps in the development of clusters of NaCl, or more correctly clusters of $Na^+(NaCl)_n$ with one excess sodium ion (the reason for the excess sodium atom will be discussed at the end of this section). The structures shown in that figure come from a theoretical calculation using a two-body interaction potential of the form

$$V_{ij}(r_{ij}) = \frac{Z_i Z_j}{r_{ij}} + A \exp(-r_{ij}/\varphi) \qquad (1)$$

where the second term is repulsive, and the first one is purely coulombic, repulsive or attractive depending on the nature of the two interacting ions. r_{ij} is the distance between the ions, Z_i, Z_j are the

charges of the ions and A and φ are appropriate constants.

The embryonic growth appears to terminate with the thirteen cluster, which essentially is identical with the unit cell of the macroscopic crystal. This is a very short life span of a rock salt embryo. In general, however, salts are not really so simple.

Instead of NaCl one may study CsI or CuBr. All the three salts are predicted to have the same embryonic forms up to size thirteen, which invariably takes the shape of a face centered cubic unit cell[3]. What makes this result nontrivial is the fact that CsI is body centered cubic in its macroscopic form like the CsCl crystal, while CuBr in bulk has a crystal structure of zinc blende. The situation is illustrated in Fig. 1 (of this Lecture). The rock salt form appears to be energetically favored at the early stages of growth of not only NaCl but also CsI and CuBr. Consequently, the two systems CsI and CuBr are not at all at the end of their embryonic development at size n=13. It remains a subject for future research to find out how far the growth spiral goes in the cases of CsI and CuBr. At any rate, the ionic compounds are examples of pure particle order.

If an intense beam of high-energy (5 keV) Xenon ions (Xe^+) is directed against a solid surface (e.g. CsI), secondary ions are ejected from the surface and can be detected in a mass spectrometer. These secondary ions include not only simple, ionized molecules but also large clusters. A mass spectrum of $[Cs(CsI)_n]^+$ clusters produced in this way is shown in Figure 2. The peak corresponding to n = 13, that is, to the cluster $[Cs_{14}I_{13}]^+$ is particularly strong[2]. Analogous clusters produced from NaCl and CuBr, that is, $[Na_{14}Cl_{13}]^+$ and $[Cu_{14}Br_{13}]^+$ respectively, also have an enhanced stability. Since these clusters are too small to be observed directly, theoretical considerations are required in order to

determine their structure. Total energy calculations using a two-body interatomic potential indicate that $[Cs_{14}I_{13}]^+$ has more than the usual binding energy. This is shown in Fig. 3 for the case RbCl. The curve is rather smooth except for $[Cs_{14}I_{13}]^+$. The reason for this is understood by looking at the structure of this cluster (fig. 1). $[Cs_{14}I_{13}]^+$ Is highly symmetric, resembling a portion of the rock-salt structure. The same explanation holds for the enhanced stability of $[Na_{14}Cl_{13}]^+$ and $[Cu_{14}Br_{13}]^+$

The other significant features in the mass spectrum of fig. 2 are a sharp decrease in the intensity just after n = 22, 37 and 62. The analysis of n = 13 suggests that these additional features can be explained by an enhanced stability of clusters with very symmetric forms. These forms, again a piece of a perfect rock-salt crystal, have been plotted in the Figure.

We now turn to the question why we have concentrated on clusters with formula $[M(M_nX_n)]^+$ and not $[M_nX_n]^+$. To see the reason we show in Figure 4 the relative yield of Cesium Subchloride clusters formed by quenching Cs vapour in a mixture of He and Cl_2 (ref. 3). The top curve indicates that if only one Cl atom is incorporated into the cluster , mass peaks corresponding to $[Cs_2Cl]^+$, $[Cs_4Cl]^+$, $[Cs_6Cl]^+$, $[Cs_8Cl]^+$, etc., are particularly strong. However, if two Cl atoms are incorporated into the cluster, and odd number of Cs atoms are preferred, i.e., the peaks $[Cs_3Cl_2]^+$, $[Cs_5Cl_2]^+$, $[Cs_7Cl_2]^+$, etc., are strong. Inspection of the entire series of curves in Fig. 4 reveals that, if the number of Cs atoms plus the number of Cl atoms is odd, the peak in the mass spectrum is strong. This result can be understood by considering three effects, which

together cooperate to give the observed mass spectra. Take first the case of $(Cs_nCl)^+$ clusters (top curve). First of all the single chlorine atom will form a Cl^- ion. This leaves n-1 free electrons in the cluster. After that, ionization leaves the cluster with n-2 free electrons. These electrons are subject to spin-pairing effects, already discussed in Lecture 3 of this Series for the case of pure alkaline clusters. Consequently $(Cs_nCl)^+$ clusters with n-2 even will be more stable than clusters with n-2 odd. This is what the mass spectrum shows. For the next curve, which corresponds to $(Cs_nCl_2)^+$ clusters, the number of free electrons in n-3, since there are now two chlorine atoms in the cluster. Then, clusters with n-3 even are more stable than those will n-3 odd. This argument explains the oscillations seen in Fig. 4. Finally we observe that the most stable cluster in each curve contains exclusively ions with rare gas electronic configurations: $(Cs_2Cl)^+$, $(Cs_3Cl_2)^+$, $(Cs_4Cl_3)^+$, $(Cs_5Cl_4)^+$, $(Cs_6Cl_5)^+$. As the partial pressure of chlorine is increased the mass pectrum simplifies considerably. A series of strong peaks emerges corresponding to clusters with composition $[M(MX)_n]^+$. In fact, we have concentrated our discussion on these clusters in the first part of this section.

3. CARBON CLUSTERS[1,4,5]

The structures of carbon clusters are good examples of the synthesis of wave and particle order that one finds in covalent compounds. This synthesis creates beautifully structured molecules.

The first laser evaporation experiments, performed by Rohlfing et al[6] observed carbon clusters in the 40- to 300- atom mass range. Remarkably, only the even-numbered clusters were present as though

some unknown process in the supersonic nozzle sensed the "evenness or oddness" of each cluster and removed the odd (see Figure 5). Experiments have shown that C_N clusters with 24, 28, 32, 36, 50, 60 and 70 atoms have enhanced stability. The C_{60} cluster attracts special interest. As seen in Fig. 5A, over the mass range detected in this experiment C_{60} accounts for more than 50% of all the clusters observed. Its conjectured struture is given in Fig. 6 (refs. 4, 5). By placing atoms at each vertex of a truncated icosahedron, one generates a pattern of bonds generally familiar as the pattern of seams of a soccerball. This is an excellent solution to the problem of forming a surface with the vacuum while satisfying the valency demands of all atoms. The structure has twenty hexagonal rings, as known form benzene and form graphite (fig. 6) and twelve pentagons. It can be viewed as a hexagonal graphitic sheet, which, by incorporating pentagons, has been able to curl into a ball, perfectly tying up all dangling bonds. A key aspect contributing to the unique stability of this structure is the fact that, by symmetry, the truncated icosahedron arranges the maximum possible number of atoms uniformly on the surface of a sphere. As a consequence, the strain of distorting what would ordinarily be a planar conjugated double-bond system in then distributed with perfect evenness. Leonardo da Vinci first studied this structure in the early sixteen century.

The structure proposed in Fig. 6 is only one of an infinite number of possible closed nets composed of five and six-membered rings. Starting with C_{20} (in the form of a dodecahedron) and with the sole exception of C_{22}, any large even-numbered carbon cluster can be formed into a closed network. By means of a theorem attributed to Euler it can be shown that all such structures must have exactly 12 five-membered rings. As an

example, Fig. 7 shows a possible closed spheroidal net structure for C_{72}. Such closed spheroidal structures for the even-number carbon clusters have come to be called "fullerenes" of which C_{60} is prototypical.

Note that, unlike the carbons in C_{60}, the carbon atoms in the C_{72} fullerene structure of Fig. 7 are not all equivalent. In general, for all fullerenes the strain of closure tends to concentrate at the vertices of the pentagons. Only for C_{20} and C_{60} can this strain be distributed uniformly over all atoms. To first order the net strain of closure in constant independent of the fullerene size[4]; hence the average strain per carbon atom will increase as the cluster gets smaller. The C_{20} dodecahedron would probably be too highly strained as a bare molecule (although the hydrogen-saturated $C_{20}H_{20}$ is a known and very stable species). Electronic structure calculations have estimated that the closed fullerene structures begin to be more stable than the alternative open graphite sheet somewhere in the C_{30} to C_{40} region . The calculations would then predict that somewhere in the cluster distribution above C_{30} one might begin to observe the fullerenes.

The "evenness" of the large carbon cluster distribution seen originally may result from the fact that only the even-numbered clusters can close to form a fullerene. Odd-numbered clusters can begin to curl so as to tie up dangling bonds, but there will always be at least one atom in such a cluster with a remaining dangling bond. The odd-numbered clusters would then be too reactive to survine long in a condensing carbon vapor. Supersonic beam experiments probing the reactivity of carbon clusters have verified this: all small clusters and large clusters with odd N are highly reactive. In contrast, C_{60} and all even-N clusters with $N > 40$ are virtually inert, in good agreement with the suggestion that they are closed fullerenes.

Simply by considering the placement of the pentagonal rings and the degree to which strain is concentrated at any particular atom, it is possible to explain why some members of the fullerene distribution such as C_{70} and C_{50} should be specially stable as well. These points are discussed in detail by Kroto[5].

The same principles can be used to construct very stable cage-like structures bigger than C_{60} starting from larger icosahedra. C_{240} and C_{540} are the second and third members of the series. So far, only the first member of the series, C_{60}, is experimentally well characterised. These structures are so perfect, an close so beautifully into themselves, that they seem destined to arrest the growth process rather than furthering it. Al least a major shake-up of the whole structure in likely to be required at each step. This kind of covalent molecules are very stable entities. It may be possible to arrange them in homologous series of increasing size, but bringing about growth requires considerable chemical skill. It has been proposed that C_{60} clusters are responsible for some features in the absorption spectra of interestelar matter. Also, great expectations exists for encapsulating atoms in C_{60} cages.

Nevertheless, soot particles do form, for instance in a burning candle. Figure 8 illustrates and imaginative hypothesis of how this may occur[5]. Combining hexagons and pentagons a bit at random will produce curled-up structures like snail shells. The exposed edge will allow further growth as long as there is seed material present and the temperature is high enough. Such a picture of the growth process lies nearer to the world of those clusters that play a role in practical life.

The chemical reactivity of C_{60}^+ has been probed by exposing it to neutral reactant gas over a set time period. Evidence for reaction can be

sought by looking both for the depletion of the C_{60}^+ parent ion signal and for the appearance of new mass peaks corresponding to reaction products. As with neutral reaction studies, not only C_{60}^+ but all the fullerene ions were found to be completely unreactive in presence of such reactive gases as O_2, NH_3 or NO. No evidence of reaction was ever detected. The fullerenes are extremely inert clusters.

One of the most useful probes of any new cluster species is to see how it fragments upon laser excitation. The results of such experiment for all the positive carbon clusters up to over 70 carbon atoms reveal new aspects of these clusters that were quite unexpected but that turn out to be fully in accord with the fullerene model.

When any carbon cluster ion with $N < 31$ is irradiated with ultraviolet light, the clusters fragment and a single primary fragmentation route is followed: loss of C_3 (quantum chemical calculations indicate, indeed, that C_3 is a particularly stable cluster). However, starting at C_{32}^+, the photodissociation process changes drastically for all higher clusters. The large even-numbered clusters (the fullerenes) are extremely difficult to photodissociate. When ultimately they are irradiated with sufficient laser intensity to begin to fragment, they do so by the loss of C_2. This is surprising because C_2 is much less stable than C_3. Interestingly, C_{32}^+ acts as a sharp dividing line: for all lower clusters only C_3 loss in observed, whereas all higher even-numbered clusters lose C_2 and all higher odd-numbered clusters lose C_1. C_{60}^+ is by far the most difficult to photodissociate. As higher laser fluences are used on any particular mass-selected fullerene, the C_2 loss process appears to continue in successive steps. With sufficiently intense laser excitation this loss continues, but it breaks off abruptly at C_{32}^+.

These photofragmentation results constitute a stringent test for any model of the structure of C_{60}^+ and the other large clusters. The fullerene model passes this test if one invokes a concerted C_2 loss mechanism in which the next smaller cage is formed as the C_2 leaves. Upon further C_2 loss, the fullerene cage becomes increasingly strained. Ultimately the C_2 loss process would be expected to terminate abruptly as the final fullerene cage becomes so strained that it shatters. This is precisely the behavior exhibited at C_{32}^+.

The critical point where the cage bursts is affected if a fairly large metal atom is placed inside. Fig. 9 shows evidence that this is what happens. Here a $C_{60}K^+$ cluster has been trapped in the apparatus along with a similar amount of the C_{64}^+ bare fullerene ion. Fig. 9 shows the results of irradiating these species with an ArF excimer laser. The bare fullerene fragments seen here originated from the C_{64}^+ parent. Like the bare fullerenes, $C_{60}K^+$ is highly photoresistant, and when it fragments it does so by C_2 loss producing first $C_{58}K^+$, then $C_{56}K^+$, and so forth. The bare fullerene fragment distribution extends down through C_{32}^+, while the C_nK^+ fragments break off abruptly at $C_{44}K^+$. For a similar experiment with $C_{60}Cs^+$ (a large metal atom) the break in C_nCs^+ fragment distribution occurs at $C_{48}Cs^+$.

We finally mention that the main facts of the fullerene picture are suported by simulated annealing calculations using a semiempirical many-body potential[8].

REFERENCES

1. S. Bjornholm, Contemp. Phys. 31, 309 (1990)
2. T.P. Martin, Angew. Chem. Int. Ed. Engl. 25, 197 (1986)
3. T.P. Martin, Phys. Rept. 95, 167 (1983)
4. R.F. Curl and R.E.Smalley, Science 242, 1017 (1988)
5. H. Kroto, Science 242, 1139 (1988)
6. E.A. Rohlfing, D.M. Cox and A. Kaldor, J. Chem. Phys. 81, 3322 (1984)
7. K. Ragavachari and J.S. Binkley, J. Chem. Phys. 87, 2191 (1987)
8. P. Ballone and P. Milani, Phys. Rev. B 42, 3201 (1990)

FIGURE CAPTIONS

Figure 1. Calculated cluster structure of the salts $[M_{14}X_{13}]^+$ with MX either NaCl, CsI or CuBr, respectively. The three clusters exhibit the same structure, although the bulk crystals are known to belong to three different crystallographic classes (right-hand side)

Figure 2. Size distribution of $[Cs(CsI)_n]^+$ clusters determined by secondary mass spectrometry[2]. The numbers in parantheses indicate the sizes of perfect, rectangular clusters.

Figure 3. Binding energy per MX unit for the most stable forms of positively charged clusters.

Figure 4. The yield of cesium subchloride clusters formed by quenching Cs vapor in a mixture of He and Cl_2. Noteworthy is the vertical and horizontal alternation in the amount of cluster formed. The filled circles correspond to clusters containing ions with rare gas electronic configuration (ref. 3).

Figure 5. Mass spectra of carbon cluster distribution in a supersonic beam produced by laser vaporization under conditions of increasing extent of clustering (C to A).

Figure 6. The truncated icosahedron (football structure) ascribed to the exceptionally stable C_{60} (ref. 4). The structures of the benzene molecule and graphite is also shown.

Figure 7. A. possible fullerene structure for the cluster C_{72}.

Figure 8. The growth of a soot particle, as suggested by Kroto and McKay[5].

Figure 9. Low mass portion of the daughter ion fragments produced by intense laser excitation of $C_{60}K^+$.

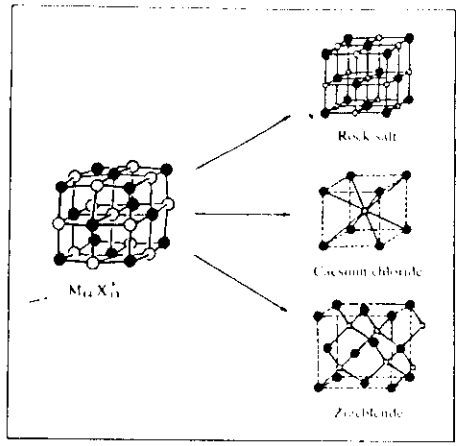

Figure 1. . Calculated cluster structure for the salts $M_{14}X_{13}$, with MX either NaCl, CsI or CuBr, respectively. The three salts exhibit the same cluster structure, although the bulk crystals are known to belong to three different crystallographic classes as shown on the right-hand side.

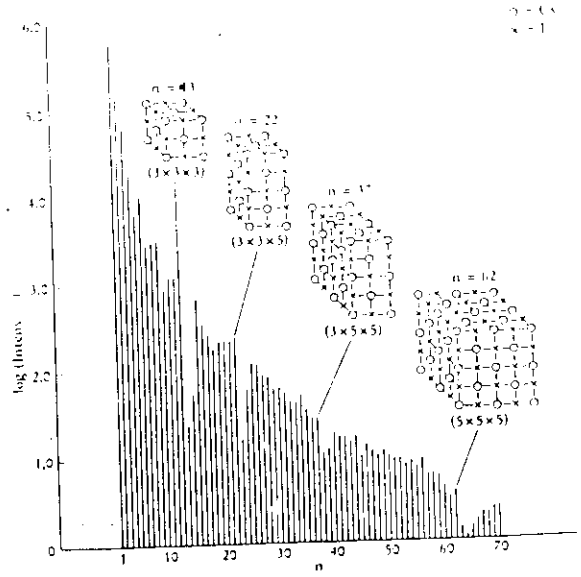

Fig 2

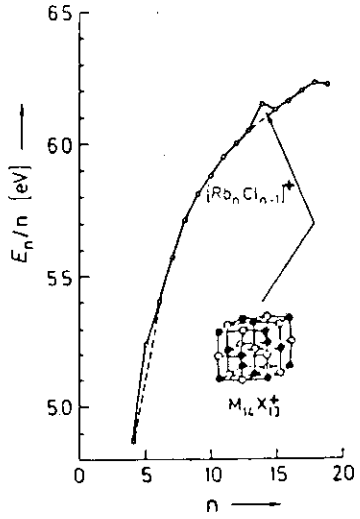

Fig. 3. Binding energy per MX unit for the most stable forms of positively charged clusters.

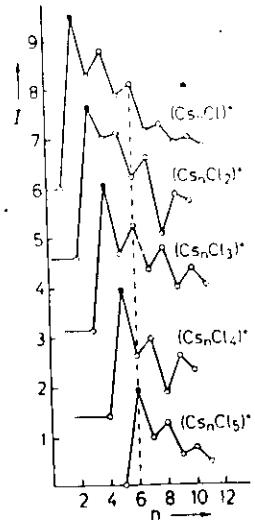

Fig. 4. The yield of cesium subchloride clusters formed by quenching Cs vapor in a mixture of He and Cl_2. Noteworthy is the vertical and horizontal alternation in the amount of cluster formed. The filled circles correspond to clusters containing ions with rare gas electronic configurations.

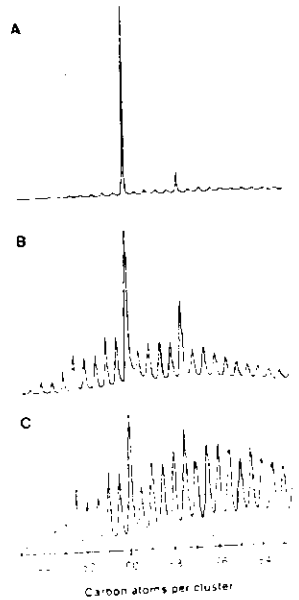

Fig. 5. Mass spectra of carbon cluster distributions in a supersonic beam produced by laser vaporization under conditions of increasing extent of clustering (C to Ar).

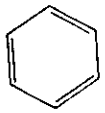

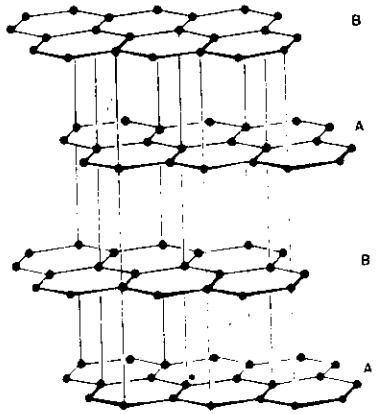

The structure of hexagonal graphite.

Truncated icosahedral structure proposed for C_{60}

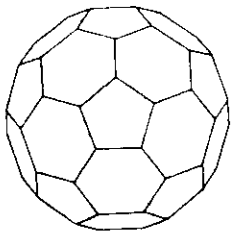

Fig 6

Fig. 7. A possible fullerene structure for the cluster C_{72}.

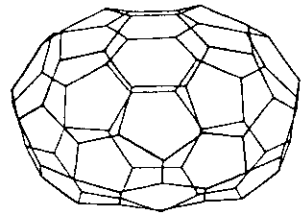

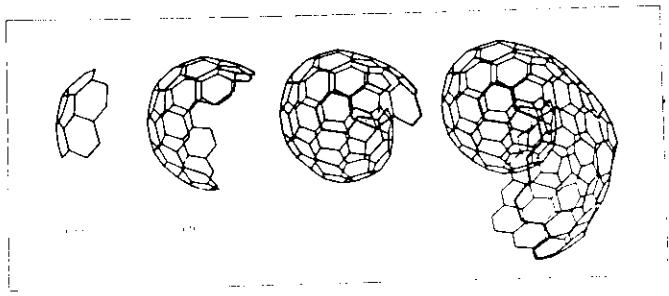

Figure 8. The growth of a soot particle, as suggested by Kroto and McKay

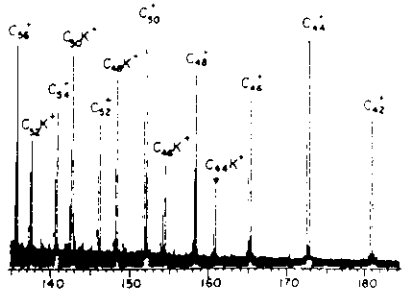

Fig 9